RBMO

ELSEVIER

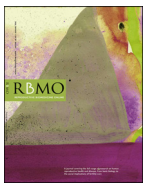

ARTICLE

Endometrial protein expression and phosphorylation landscape decipher aberrant insulin and mTOR signalling in patients with recurrent pregnancy loss

BIOGRAPHY

Chao Chen is a postgraduate student at the Centre for Reproductive Medicine, Department of Obstetrics and Gynecology, Peking University Third Hospital (China). Her work focuses primarily on the study of proteins associated with the endometrium, and their functional mechanisms and structural analysis.

Chao Chen[a,b,c,d,†], Qi Wen[a,b,c,d,†], Feng Deng[a], Rong Li[a,b,c,d], Ying Wang[a], Xiumei Zhen[a,*], Jing Hang[a,b,c,d,*]

KEY MESSAGE

Proteomic and phosphoproteomic profiling revealed dysregulated insulin/cAMP and AMPK/mTOR signalling in the endometrium of women with recurrent pregnancy loss (RPL), accompanied by altered expression of four proteins: PRKAR1B, ADCY3, PRKAA2 and LPIN2. These findings provide new insights into the pathogenesis of RPL, and help identify potential targets relevant to its treatment.

ABSTRACT

Research question: What are the proteomic and phosphoproteomic differences between the endometrium of women with recurrent pregnancy loss (RPL) and the endometrium of healthy control women during the proliferative and secretory phases of the menstrual cycle?

Design: In total, 54 endometrial samples were collected during the proliferative and secretory phases from women with RPL ($n = 28$) and healthy controls ($n = 26$). Comprehensive proteomic and phosphoproteomic analyses were conducted using label-free liquid chromatography-tandem mass spectrometry ($n = 44$), and verified through Western blotting ($n = 10$). Three comparison groups were established: total RPL endometrium versus total control endometrium; RPL proliferative endometrium versus control proliferative endometrium; and RPL secretory endometrium versus control secretory endometrium.

Results: Differentially expressed proteins and differentially phosphorylated proteins were identified in the three comparison groups. Combining pathway enrichment, network analysis and soft clustering analysis, the insulin/cyclic nucleotide signalling pathway and AMPK/mTOR signalling pathway were identified as the major contributors to the aberration of RPL endometrium. Western blotting verified altered expression of four proteins: cAMP-dependent protein kinase type I-β regulatory subunit, adenylate cyclase type 3, 5′-AMP-activated protein kinase catalytic subunit α-2 and phosphatidate phosphatase LPIN2.

[a] Centre for Reproductive Medicine, Department of Obstetrics and Gynaecology, State Key Laboratory of Female Fertility Promotion, Peking University Third Hospital, Beijing, China
[b] Key Laboratory of Assisted Reproduction (Peking University), Ministry of Education, Beijing, China
[c] National Clinical Research Centre for Obstetrics and Gynaecology, Beijing, China
[d] Beijing Key Laboratory of Reproductive Endocrinology and Assisted Reproductive Technology, Beijing, China
† These authors contributed equally to this work.

*Corresponding authors. E-mail addresses: xmzhen1970@aliyun.com (X. Zhen), hangjbysy@163.com (J. Hang). https://doi.org/10.1016/j.rbmo.2023.103585 1472-6483/
Declaration: The authors report no financial or commercial conflicts of interest.

KEY WORDS

RPL
Endometrium
Proteomics
Phosphoproteomics
mTOR signalling pathway
Insulin signalling pathway

Conclusions: This exploratory study provides insights into the differentiated protein expression and phosphorylation profiles of the endometrium of women with RPL in both the proliferative and sectretory phases of the menstrual cycle. The results highlight potential proteins associated with the pathogenesis of RPL that may serve as potential indicators for RPL. The findings contribute to the identification of potential targets for RPL treatment as well as its pathogenesis.

INTRODUCTION

Recurrent pregnancy loss (RPL), also referred to as recurrent miscarriage and recurrent spontaneous abortion, is a considerable reproductive disorder affecting approximately 1–4% of couples (*Dimitriadis et al., 2020*; *Jauniaux et al., 2006*), with increasing prevalence in recent years. The condition is characterized by two or more consecutive pregnancy losses prior to 24 weeks from the last menstrual period (*ESHRE Guideline Group on RPL, 2018*). Common causes of RPL including congenital or environmental factors have been identified, such as various genetic, anatomical, uterine endocrinologic, immunologic, thrombophilic and endometrial risk factors (*Alecsandru et al., 2021*; *Carbonnel et al., 2021*; *de Ziegler and Frydman, 2021*; *Klimczak et al., 2021*; *Pirtea et al., 2021*). However, these causes only account for approximately 40% of cases, with the rest remaining unexplained (*El Hachem et al., 2017*). Women with RPL are treated empirically with progesterone supplementation, anticoagulation and/or immunomodulation rather than targeted therapy, and predicting the occurrence of failed pregnancies before gestation using hysteroscopy biomarkers is currently impractical. Therefore, understanding the pathogenesis of RPL is crucial to improve the diagnosis and treatment of patients.

The endometrium, as the soil for embryonic implantation and placental formation, permits a framework for embryo–maternal interactions (*Critchley et al., 2020*). It undergoes extensive cyclic modifications during each menstrual cycle, consisting of menstruation, proliferative and secretory phases (*Salamonsen, 2019*), with decidualization occurring during the mid-secretory phase (typically days 20–22). Dysfunction of this phase can impair fetal intrauterine growth and cause RPL (*Gellersen and Brosens, 2014*; *Salker et al., 2010*). Consequently, there is an urgent need for a full interpretation of endometrial regulation and how its aberrance contributes to RPL.

Previous studies have investigated the DNA methylome, transcriptome and microRNA expression associated with the pathogenesis of RPL (*Bahia et al., 2020*; *Yu et al., 2018*; *Zhou et al., 2021*), and others have focused on the endometrial immune environment in RPL, including exploration of the single-cell decidual immune landscape (*Chen et al., 2021*; *Guo et al., 2021*; *Huang et al., 2021*; *Wang et al., 2021*). Proteomic analysis, which is able to identify proteins with adverse effects, has been used to uncover biomarkers in many diseases (*Vlahou and Fountoulakis, 2005*). Moreover, phosphorylation constitutes one of the most common post-translational modifications (PTM) of proteins (*Tarrant and Cole, 2009*), with relevant small-molecule inhibitors employed successfully in various types of disease, including cancers and cardiovascular disease (*Hua et al., 2019*; *Pfleger et al., 2019*). However, while some studies have assessed the proteomic profiles of RPL with either in-vitro cultured cells or decidua or even spermatozoa (*Bruno et al., 2020*; *Dhaenens et al., 2019*; *Naglot et al., 2021*; *Xiong et al., 2021*; *Xue et al., 2019*; *Yin et al., 2021*), their sample sizes were relatively small, and the overall PTM landscape of dysregulated endometrium in RPL remains uninvestigated. This knowledge gap greatly hinders the exploration of PTM-related pathogenesis for RPL.

Using four-dimensional label-free mass spectrometry, the present study undertook integrative proteomic and phosphoproteomic profiling of the endometrium of women with RPL during the secretory and proliferative phases of the menstrual cycle. Compared with the endometrium of control women, the endometrium of women with RPL displayed changed protein expression and phosphorylation status, and aberrant pathway enrichment in both phases. These findings could aid understanding of the pathogenesis of RPL, and provide new potential targets as clinical biomarkers. In conclusion, the overall landscape of protein expression and modification would benefit from improved understanding of endometrial function in women with RPL and exploring the potential biomarkers.

MATERIALS AND METHODS

Ethics declaration and patient recruitment

This study was approved by the Ethics Committee of Peking University Third Hospital (2016sz-007, date of approval 20 May 2016). Written informed consent was obtained from all participants. Participants were infertile patients who attended the Reproductive Medicine Centre of Peking University Third Hospital and met the indicators for hysteroscopy. RPL was defined as two or more miscarriages of unexplained aetiology. The inclusion criteria were set as follows: age <40 years; menstrual cycle of 25–35 days; and two or more miscarriages between 6 and 13 gestational weeks. Patients were excluded if they met any of the following criteria: chromosomal abnormalities; history of other gynaecological diseases; maternal anatomical abnormalities; immunological diseases; smoking; alcohol consumption; and ingestion of any chemical agent before termination of pregnancy. Age-matched women with no history of pregnancy loss were recruited for the control group. Endometrial samples were only used for analysis after infertility was confirmed to have a non-endometrial cause, such as fallopian tube obstruction. In total, 28 women with unexplained RPL and 26 fertile control women were enrolled in this study, and their detailed clinical characteristics are presented in TABLE 1.

Collection of endometrial biopsies through hysteroscopic examination

Endometrial biopsies in the secretory phase were timed between 6 and 8 days after the LH surge (days 20–22 of the menstrual cycle), and endometrial biopsies in the proliferative phase were collected on days 8–10 of the menstrual cycle. Endometrium samples from women with RPL were obtained from patients who underwent hysteroscopic examination >3 months after their last miscarriage. During hysteroscopy, the endometrial samples from each patient were obtained using a Pipelle (Lilycleaner, China), starting from the uterine fundus and moving down to the internal cervical ostium. The remaining biopsies after pathological examination were washed three times using ice-cold phosphate-buffered saline, frozen

TABLE 1 SUMMARY OF CLINICAL CHARACTERISTICS OF PATIENTS WITH RECURRENT PREGNANCY LOSS AND CONTROL PATIENTS

Characteristic	RPL (*n*=28)		Control (*n*=26)		*P*-value
Menstrual cycle phase	**RS (*n*=15)**	**RP (*n*=13)**	**CS (*n*=18)**	**CP (*n*= 8)**	
Maternal age (years)	30.33 ± 2.35	31.23 ±3 .03	31.28 ± 4.98	31.25 ± 3.73	0.883
Height (cm)	160.27 ± 3.58	162.69 ± 3.68	163.83 ± 4.68	162.75 ± 4.17	0.107
Weight (kg)	58.13 ± 7.45	62.23 ± 11.89	58.83 ± 10.03	60.88 ± 10.59	0.694
BMI (kg/m^2)	22.62 ± 2.72	23.47 ± 4.21	21.90 ± 3.48	23.11 ± 4.80	0.682
No. of gravidities	2.80 ± 0.86	2.33 ± 0.65	0.33 ± 0.69	0.13 ± 0.35	<0.001
No. of miscarriages	2.40 ± 0.83	2.23 ± 0.44	0	0	<0.001

Data are presented as mean ± SD.

P-values indicate the difference between RPL and control groups using two-tailed Student's *t*-test. Miscarriage was categorized as two or more consecutive losses before 24 weeks of gestation.

RPL, recurrent pregnancy loss; RS, RPL secretory endometrium; RP, RPL proliferative endometrium; CS, control secretory endometrium; CP, control proliferative endometrium; BMI, body mass index.

promptly in liquid nitrogen, and stored immediately at -80°C until use.

Protein extraction, digestion and phosphopeptide enrichment

Forty-four endometrial samples (RPL secretory endometrium, *n* = 10; RPL proliferative endometrium, *n* = 13; control secretory endometrium, *n* = 13; control proliferative endometrium, *n* = 8) were extracted for total protein preparation. Endometrial samples were weighed, ground into powder, and ultrasonicated with lysis buffer (8M urea, 100 mM Tris-HCl, pH 8.0, 100 mM NaCl, 1% protease inhibitor, 1% phosphatase inhibitor). The supernatant was collected after centrifugation at 12,000 *g* for 10 min at 4°C to remove the cell debris. The concentration of total protein was determined using the BCA protein assay kit (Thermo Fisher Scientific, USA).

For trypsin digestion, lysis buffer was used to adjust the protein concentration of each sample to the same volume, and equal amounts were taken for enzymatic digestion. Samples were precipitated with trichloroacetic acid at 4°C for 2 h. After three washes with ice-cold acetone, protein pellets were collected by centrifugation at 4500 *g* for 5 min, and dispersed in 100 mM tetraethylammonium bromide. After overnight digestion with trypsin in a 1:50 mass ratio, the resulting solutions were treated with 5 mM dithiothreitol for 30 min at 55°C and 11 mM iodoacetamide for 15 min at room temperature to shut the sulfhydryl group. The digested peptides were then desalted with a C18 SPE (3M, USA) column and evaporated to dryness on a CentriVap Concentrator (Labconco, USA).

To enrich the phosphorylated peptides, the above digested peptides were redissolved in 50% acetonitrile/6% trifluoroacetic acid, and incubated with pre-equilibrated immobilised metal chelate affinity chromatography microspheres (High-Select Fe-NTA Phosphopeptide Enrichment Kit). Following successive washes with buffer solutions of 50% acetonitrile/6% trifluoroacetic acid and 30% acetonitrile/0.1% trifluoroacetic acid, the bound phosphopeptides were eluted in 10% ammonium hydroxide (NH_4OH), desalted with C18 ZipTips (Millipore, USA), and vacuum-lyophilized.

Liquid chromatography-tandem mass spectrometry analysis of proteomics and phosphoproteomics

The digested peptides were dissolved in Buffer A (0.1% formic acid, 2% acetonitrile), and separated on a NanoElute Ultra Performance Liquid Chromatography system equipped with a reverse-phase analytical column (25 cm length, 100 μm i.d.). With a gradient increase of Buffer B (0.1% formic acid in 100% acetonitrile) set as 0–72 min, 7~24%; 72–84 min, 24~32%; 84–87 min, 32~80%; and 87–90 min, 80%, the peptides were separated gradually at a flow rate of 450 nl/min.

Subsequently, the peptides were ionized by capillary ion source and analysed by tandem mass spectrometry in TimsTOF Pro (Bruker Daltonics, USA) with the voltage set at 1.6 kV. The scan range of the secondary mass spectra was set at 100–1700, and the parallel accumulated sequence fragmentation (PASEF) mode was employed for data collection. Ten PASEF acquisitions of secondary spectra with parent ion charges between 0 and 5 were conducted after the collection of a primary mass spectrum. The dynamic exclusion time for tandem mass spectrometry scans was adjusted to 30 s to prevent duplicate parent ion scans.

Similarly, the enriched lysine phosphorylated peptides were separated by IonOpticks C18 reverse-phase analytical column using Buffer C (0.1% formic acid in water) and Buffer B (0.1% formic acid in 100% acetonitrile) with a 1-h linear gradient (2–22% B, 0–50 min; 22–35% B, 50–52 min; 35–90% B, 52–55 min; 90% B, 55–60 min) at a constant flow rate of 300 nl/min for phosphoproteomic analysis.

Database search

The generated raw files were processed using the MaxQuant search engine (v.1.6.6.0) in a data-dependent acquisition mode. The tandem mass spectrum was retrieved from the human SwissProt database, which added a reverse decoy database to calculate the false-discovery rate (FDR) due to random matching. The FDR values for both peptide spectrum matching and protein identification were set to 1%. The number of missed cut sites was set at 2, and trypsin was designated as the cleavage enzyme. Seven amino acid residues were chosen as the minimum peptide length, and the maximum modification number of the peptide segment was set to 5. For the first search, the main search and the second fragment

ion, the mass error tolerance for the primary parent ion was set to 20, 20 and 20 ppm, respectively. Alkylation of cysteine was designated as a fixed modification, and oxidation (methionine) and acetylation (protein N-terminal) were designated as variable modifications. Phosphorylation of serine, threonine and tyrosine were designated as variable modifications in phosphoproteomics.

Differentiated expression analysis

The horizontally normalized label-free quantitation (MaxQuant), which was divided by the mean quantification of all samples, was used as the quantitative protein intensity and the normalized value for subsequent analysis. The relative quantitative value of the modification site will be divided by the relative quantitative value of the protein corresponding to that modification site to eliminate the effect of protein expression on modification expression for phosphoproteomics analysis. For definition of differentially expressed proteins (DEP), differentially phosphorylated proteins (DPP) and differentially phosphorylation sites, the fold-change of their expression level between comparison groups was set at 1.5 (up- or down-regulated), and the *P*-value criterion, which was assessed by unpaired Student's *t*-test, for each biological replicate was set at 0.05.

Functional annotation and enrichment analysis

The subcellular localization of proteins was predicted using WoLF PSORT software. The Kyoto Encyclopedia of Genes and Genomes (KEGG) database was compared against all discovered proteins using a two-sided Fisher's exact probability test to annotate the protein pathways. This allowed for the annotation and enrichment of DEP and DPP. Using the Benjamini–Hochberg correction, the obtained *P*-values were further modified to account for multiple testing, and a corrected *P*-value <0.05 was considered significant. The UniProt-GOA database (http://www.ebi.ac.uk/GOA/) was used to create the gene ontology annotation.

Functional enrichment clustering

Hierarchical clustering was employed using the Fisher's exact test *P*-value from the enrichment study to group similar functions in various comparison groups together and depict them on a heatmap. Different comparison groups were represented horizontally on the heatmap, while associated functions (gene ontology categories or KEGG) that were enriched by differentially expressed changed proteins in various comparison groups were represented vertically.

Protein–protein interaction network analysis

Information for protein–protein interactions (PPI) was obtained from the STRING protein interaction network database (Version 11.0) by matching the database numbers or protein sequences of DEP and DPP in different groups with a confidence level ≥ 0.7. The differentially modified protein interaction network was then visualized using the R package 'networkD3' tool.

Mfuzz soft clustering

The relative expression of proteins identified by quantitative proteomics was transformed using a Log2 logarithm and then screened for SD >0.5. The remaining proteins after screening were used for expression pattern clustering analysis by the Mfuzz method (*Kumar and Futschik, 2007*) (RRID:SCR_000523). The degree of clustering ambiguity (m) was set at 2 for Mfuzz analysis, and the number of clusters (k) was adjusted accordingly to ensure the expression tendency remained consistent within each cluster. Subsequently, KEGG pathway enrichment analysis was performed on DEP and DPP after Mfuzz analysis in different comparison groups. The analysis was performed by Fisher's exact test, and was considered significantly enriched for *P*-values <0.05.

Kinase activity prediction

The site-specific kinase-substrate regulations were predicted using iGPS1.0 (v1.0) software. PPI information was applied as the major background factor to deposit the potentially false-positive hits. Next, the Gene Set Enrichment Analysis method was used to predict kinase activities. Kinase activity scores were measured using normalized enrichment scores, which were derived using the enrichment analysis approach. With a significant enrichment of *P*-values <0.05, kinase activity was regarded to be activated when the score was >1 and inhibited when the score was <1.

Kinase-pathway network analysis

The relationship between phosphorylated kinases and substrate modifications was explored using a kinase functional network that links kinase signalling to KEGG pathway dysregulation through phosphorylation sites and phosphoproteins. Nodes represent significantly differential proteins, differential phosphosites, enriched kinases and enriched KEGG pathways. Connected edges contain enriched kinases, up- or down-regulated phosphosites connecting to corresponding regulated proteins, and proteins connecting to enriched KEGG pathways. Networks were visualized using Cytoscape (RRID:SCR_003032).

Western blot

Frozen human endometrial tissues were homogenized in 500 μl of 1 × RIPA buffer (Applygen, China) supplemented with protease inhibitor and phosphatase inhibitor cocktails. The resultant supernatants were collected after samples were centrifuged at 13,523 *g* for 10 min at 4°C. Twenty micrograms of the total protein of each sample was separated by SDS-PAGE electrophoresis and transferred to polyvinylidene fluoride membranes (IPVH00010, Millipore). The membranes were blocked with 5% (w/v) skimmed milk (232100, BD) at room temperature for 1 h and then incubated with the primary antibodies against cAMP-dependent protein kinase type I-β regulatory subunit (PRKAR1B; Abcam Cat# ab167325, RRID:AB_3073550), adenylate cyclase type 3 (ADCY3; Abcam Cat# ab125093, RRID:AB_10975307), 5′-AMP-activated protein kinase catalytic subunit α-2 (PRKAA2; Abcam Cat# ab97275, RRID:AB_10695947), phosphatidate phosphatase LPIN2 (LPIN2; Abcam Cat# ab176347, RRID:AB_2924332) and glyceraldehyde 3-phosphate dehydrogenase(P01L01, Gene-Protein Link) overnight at 4°C. The membranes were then washed three times with TBS-T buffer [25 mM Tris, pH 8.0, 150 mM NaCl and 0.05% (w/v) Tween-20] and incubated with horseradish-peroxidase-conjugated secondary antibody (1:5000) for 1 h at room temperature. After three washes with TBS-T buffer, protein intensities were visualized under the chemiluminescence imaging analysis system (Tanon, China). The grayscale of Western blotting was analysed using ImageJ.

Statistical analysis

GraphPad Prism 9.0 was applied for statistical analyses and graphics generation. Data are shown as mean ± SD. The comparison between RPL and control groups in **TABLE 1** was performed using two-tailed Student's *t*-test, as well as the analyses for protein expression and phosphorylation. A *P*-value <0.05 was considered to indicate significance.

RESULTS

Overview of protein expression and phosphorylation of endometrium of women with RPL

The menstrual cycle can be divided into three phases: the menstruation phase, the proliferative phase and the secretory phase (FIGURE 1A). To investigate the periodic variation of women with RPL and identify potential biomarkers associated with this disorder, 28 women with RPL and 26 matched fertile controls were recruited in this study (FIGURE 1B). Women with RPL exhibited a significantly higher pregnancy loss rate compared with the control group ($P < 0.001$) (TABLE 1). According to the menstrual cycle, endometrial biopsies were taken from the RPL and control groups during both the proliferative and secretory phases, resulting in two RPL groups (RPL proliferative endometrium and RPL secretory endometrium) and two control groups (control proliferative endometrium and control secretory endometrium). These four group samples were then subjected to label-free liquid chromatography-tandem mass spectrometry analysis with or without phosphor-peptide enrichment (FIGURE 1B). With the detection of one or more unique peptides and FDR set to 1%, 7123 polypeptides and 3693 phosphopolypeptides were quantified with high confidence values in proteomics and phosphoproteomics, respectively (Supplementary Figure S1). These quantifiable polypeptides and phosphopolypeptides were used for subsequent analysis. Three comparison groups were established to clarify differences in multiple aspects: total RPL endometrium compared with total control endometrium, RPL proliferative endometrium compared with control proliferative endometrium, and RPL secretory endometrium compared with control secretory endometrium. DEP and DPP for the three comparison groups were calculated (FIGURE 1C–D and Supplementary Tables 1–6). The results showed that the number of DPP was greater than the number of DEP; for example, only 47 proteins were differentially expressed, while 844 proteins were differentially phosphorylated in the total RPL endometrium versus total control endometrium group, indicating that PTM may play a more extensive role in regulating endometrial function.

The traditional differential expression analysis, which is normally applied for comparison between two groups, has limitations in interpreting multiple groups. To overcome the discrepancy caused by diverse menstrual phases, a fuzzy c-means algorithm using Mfuzz was used to analyse all samples systematically (*Kumar and Futschik, 2007*). Several values were used to analyse protein expression trends in the three comparison groups, and one cluster ($n = 15$) was found to be consistently well clustered with lower expression in RPL proliferative endometrium compared with control proliferative endometrium but higher expression in RPL secretory endometrium compared with control secretory endometrium (data not shown). By adopting $k = 4$, the subsequent KEGG pathway analysis displayed that this cluster (Cluster 2) was associated with the mTOR signalling pathway and steroid hormone biosynthesis (Supplementary Figure 2A). Similarly, the clustering of phosphor proteins showed that Cluster 1 ($n = 346$) was consistently clustered, and was associated with the Wnt signalling pathway and cell cycle (Supplementary Figure 2B). These results suggest that abnormalities in the mTOR signalling pathway and Wnt signalling pathway may be associated with abnormal endometrial function in women with RPL.

Identification of proteins associated with mTOR signalling and cyclic nucleotide signalling in the secretory endometrium of women with RPL

As implantation and decidualization occur in the mid-secretory phase or mid-luteal phase, the difference between RPL secretory endometrium and control secretory endometrium was compared first. The subcellular locations of DEP were distributed extensively in the nucleus, plasma membrane and cytoplasm (FIGURE 2A). To further understand the

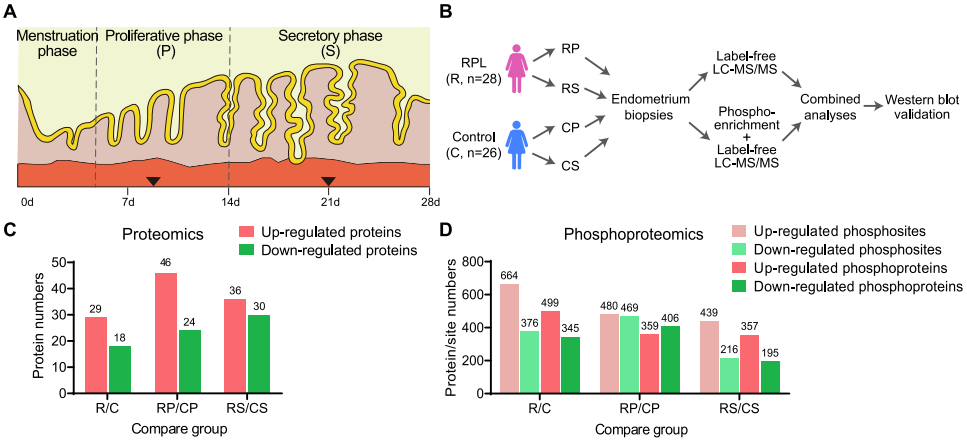

FIGURE 1 Profiling of the proteome and phosphoproteome of the endometrium of women with recurrent pregnancy loss (RPL) and healthy controls. (A) Schematic diagram of the endometrium under different menstrual cycle phases. Black arrowheads indicate the collection time points of the endometrial samples. (B) Experimental design for proteomic and phosphoproteomic analysis of endometrial biopsies. The graphical pipeline of endometrial sample collection, peptide or phosphopeptide enrichment, quantitative mass spectrometry protocol, bioinformatics analysis and experimental validation. Liquid chromatography-tandem mass spectrometry (LC-MS/MS) identification of (C) proteomic database for differentially expressed proteins and (D) phosphoproteomic database for differentially phosphorylated sites and proteins. Student's *t*-test was applied to distinguish the expression difference between different comparison groups. Three comparison groups were used: R/C, total RPL endometrium versus total control endometrium; RP/CP, RPL proliferative endometrium versus control proliferative endometrium; RS/CS, RPL secretory endometrium versus control secretory endometrium; P, proliferative phase; S, secretory phase.

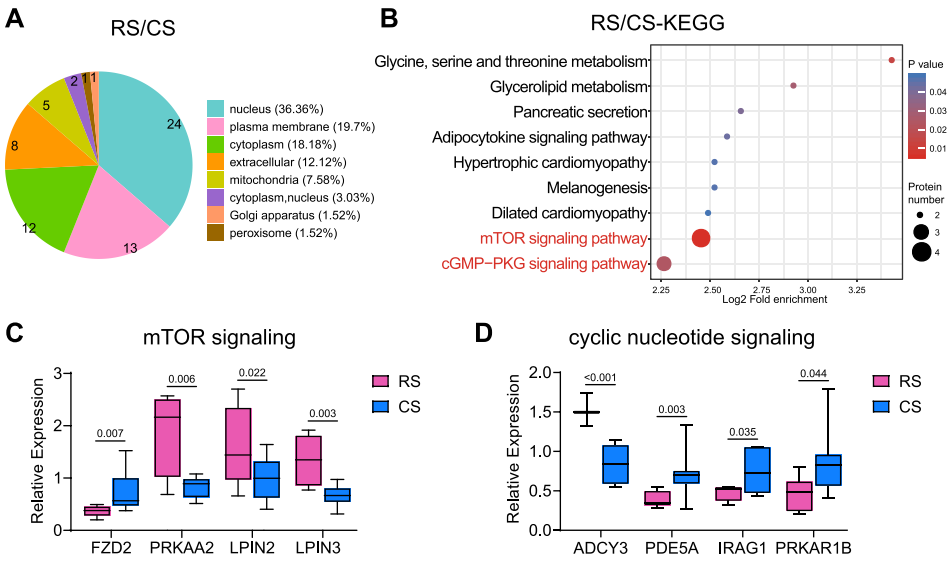

FIGURE 2 Quantitative proteomic study identifies cyclic nucleotide alteration in the secretory phase of endometrium of women with recurrent pregnancy loss (RPL). (A) Subcellular localization prediction of differentially expressed proteins (DEP) in RPL secretory endometrium (RS) versus control secretory endometrium (CS) using WoLF PSORT software. (B) Kyoto Encyclopedia of Genes and Genomes pathway enrichment analysis identification of important pathways dependent on DEP identified in comparison between RS and CS. The colour blocks corresponding to functional classification indicate the magnitude of enrichment, displayed with colours ranging from blue (weak enrichment) to red (strong enrichment). (C) Relative normalized expression of Frizzled-2 (FZD2), 5′-AMP-activated protein kinase catalytic subunit α-2 (PRKAA2), phosphatidate phosphatase LPIN2 (LPIN2) and phosphatidate phosphatase LPIN3 (LPIN3), which are involved in mTOR signalling, from mass spectrometry data. (D) Relative normalized expression of adenylate cyclase type 3 (ADCY3), cGMP-specific 3′,5′-cyclic phosphodiesterase (PDE5A), inositol 1,4,5-triphosphate receptor associated 1 (IRAG1) and cAMP-dependent protein kinase type I-β regulatory subunit (PRKAR1B), which are involved in cyclic nucleotide signalling. The vertical axis is represented as an expression of Log2. Student's *t*-test was applied to compare differences. The boxes represent the 25th and 75th percentiles, the central line marks the median value, and the whiskers show the upper and lower limits.

functions of these DEP, functional annotation and enrichment analysis were performed for up- and down-regulated DEP based on the KEGG database. The results showed that DEP were enriched significantly in the metabolic pathway, and the numbers of DEP for the mTOR signalling pathway and cGMP-PKG signalling pathway were the highest of the pathways identified (FIGURE 2B).

The mTOR signalling pathway has been reported to play a pivotal role in endometrial decidualization. The present results show that among all 66 DEP in RPL secretory endometrium versus control secretory endometrium comparison, four proteins in AMPK/mTOR signalling were aberrantly expressed: Frizzled-2 was reduced in the RPL group ($P = 0.007$), whereas PRKAA2, LPIN2 and LPIN3 were elevated ($P = 0.006$, 0.022, and 0.003, respectively; FIGURE 2C). Meanwhile, elevated progesterone was able to stimulate the increase in cyclic adenosine monophosphate (cAMP) and activate the downstream protein kinase A (PKA) pathway, which is closely involved in the decidualization process.

Four DEP enriched in cyclic nucleotide signalling were identified: up-regulated ADCY3 ($P < 0.001$) and down-regulated cGMP-specific 3′,5′-cyclic phosphodiesterase, inositol 1,4,5-triphosphate receptor associated 1 and PRKAR1B ($P = 0.003$, 0.035 and 0.044 respectively) (FIGURE 2D). These findings indicate that the maintenance of normal function of the secretory endometrium may be influenced by mTOR signalling and cyclic nucleotide signalling.

Additionally, the differentiated protein expression of endometrium in the proliferative phase, when self-regeneration occurs, was analysed. Gene ontology analysis revealed that the extracellular matrix was primarily affected, including regulation by collagen fibril organization in the biological process category (Supplementary Figure 3A), extracellular matrix structural constituent in the molecular function category (Supplementary Figure 3B), and collagen type VI trimer in the cellular component category (Supplementary Figure 3C). This indicates an abnormal increase in collagen deposition in women with RPL during the proliferative phase.

Protein expression clustering reveals aberrations in sugar metabolism in women with RPL

Protein expression clustering was used to gain insights into the major proteome composition of the endometrium of women with RPL. Several values were evaluated, and $k = 8$ was adopted to analyse the protein expression tendency of each cluster (FIGURE 3A). Approximately one-third of the proteins belong to clusters that exhibited similar patterns between RPL secretory endometrium/RPL proliferative endometrium and healthy controls (control secretory endometrium/control proliferative endometrium), such as Cluster 3 ($n = 200$) and Cluster 6 ($n = 170$), indicating that the expression pattern of most proteins remained unchanged between the secretory and proliferative phases in women with RPL and controls. However, the patterns of some clusters were more complicated, such as Cluster 1 which exhibited super-low expression patterns in women with RPL (RPL secretory endometrium + RPL proliferative endometrium) compared with healthy controls (control secretory endometrium and control proliferative endometrium), and Cluster 8 which

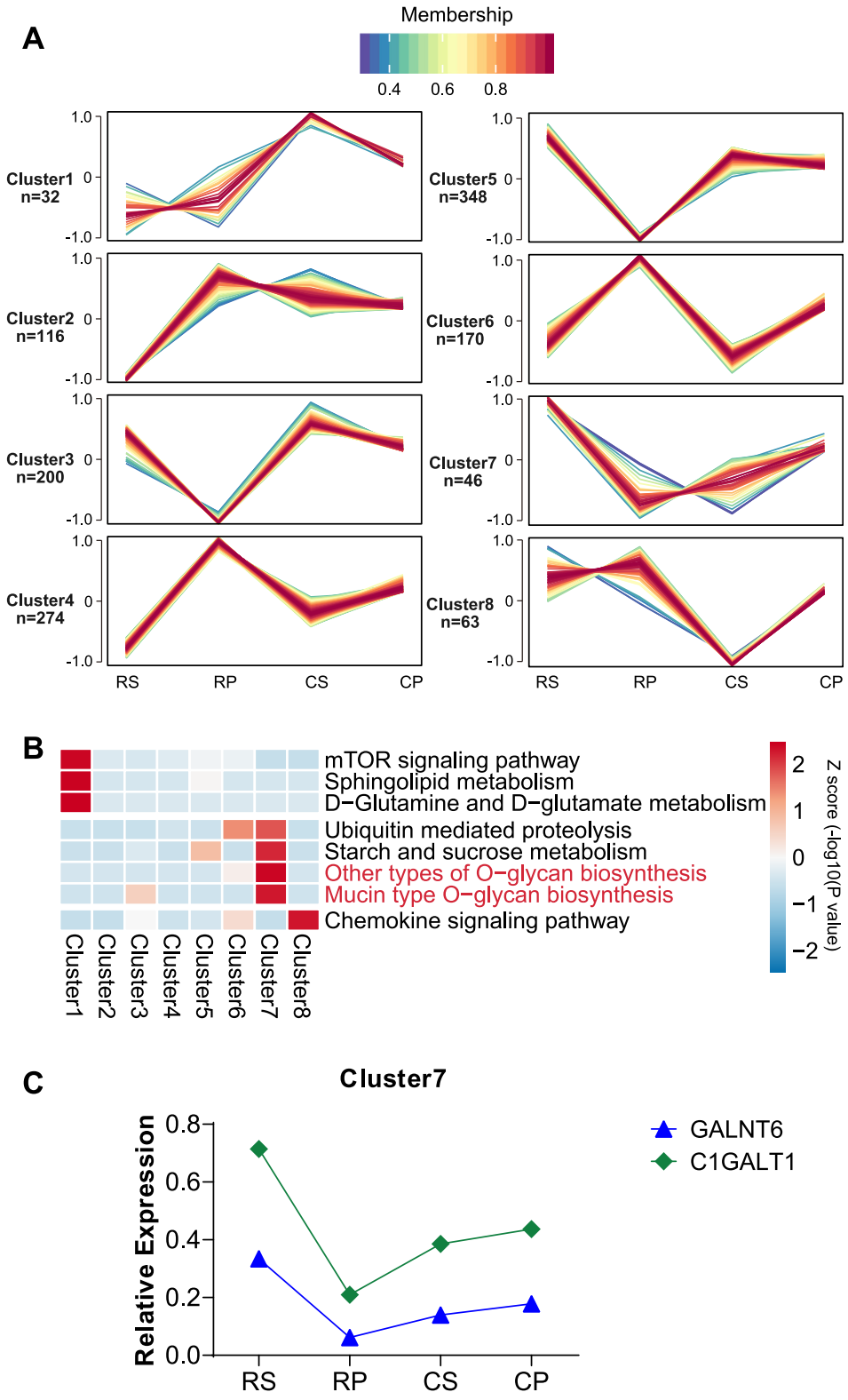

FIGURE 3 Fuzzy c-means clustering for proteomic results identifies co-regulated protein networks. (A) Line graphs show the expression tendencies of different clusters calculated by fuzzy c-means algorithm. The Y-axis refers to the relative expression changes of proteins, and the X-axis refers to samples with one broken line representing one protein. The number of clusters (*k* value) was applied as eight, and the numbers of genes in each cluster (*n* value) are shown. (B) Heatmap of Kyoto Encyclopedia of Genes and Genomes enrichment of proteins from four groups (RS, RPL secretory endometrium; RP, RPL proliferative endometrium; CS, control secretory endometrium; CP, control proliferative endometrium) with significantly enriched pathways in Clusters 1, 7 and 8 shown. (C) Relative expression pattern, from mass spectrometry data, of N-acetylgalactosaminyltransferase 6 (GALNT6) and glycoprotein-N-acetylgalactosamine 3-β-galactosyltransferase 1 (C1GALT1), which are two representative proteins in O-glycan biogenesis enriched in Cluster 7.

presented aberrant increased expression levels, especially in RPL secretory endometrium compared with control secretory endometrium (FIGURE 3A). Conversely, Cluster 7 displayed opposing behaviours between RPL secretory endometrium/RPL proliferative endometrium and control secretory endometrium/control proliferative endometrium, and enrichment analysis displayed that these highly expressed proteins in RPL secretory endometrium were significantly enriched in sugar metabolism pathways, including starch and sucrose metabolism and O-glycan biosynthesis (FIGURE 3B).

Abnormal expression patterns of two representative proteins in O-glycan biosynthesis — polypeptide N-acetylgalactosaminyltransferase 6 and glycoprotein-N-acetylgalactosamine 3-beta-galactosyltransferase 1 — were observed in RPL secretory endometrium/RPL proliferative endometrium compared with control secretory endometrium/control proliferative endometrium (FIGURE 3C). As extracellular matrix (ECM) proteins are highly glycosylated, disturbed glycosylation may impair normal ECM formation. Furthermore, decidual ECM is critical for its contact with blastocyst and subsequent trophoblast adhesion and invasion. As such, impaired ECM in the endometrium of women with RPL may result in poor development of the implanted embryo, leading to the occurrence of recurrent miscarriage. These results indicate that protein clustering analysis would comprehensively aid understanding of dynamic protein expression patterns.

Phosphoregulation network illustrates increased insulin resistance

As shown in FIGURE 1D, the difference in protein phosphorylation was more pronounced, so this study investigated how differentiated phosphorylation contributes to the occurrence of RPL. By adopting functional enrichment clustering to the molecular function category in gene ontology annotation, the up- and down-regulated phosphoproteins were analysed for all three comparison groups (FIGURE 4A). Many enriched gene ontology terms were related to either kinase binding or kinase activity, indicating a widespread regulatory phosphorylation network in the menstrual endometrium.

Next, up- and down-regulated phosphorylation in the RPL secretory endometrium versus control secretory endometrium comparison group was dissected by referring to the KEGG database. Proteins with increased phosphorylation were significantly up-regulated within insulin resistance, AMPK signalling pathway and insulin signalling pathway processes (FIGURE 4B). Meanwhile, the insulin signalling pathway was also down-regulated, together with the glucagon signalling pathway and spliceosome (FIGURE 4C). In detail, 11 up-regulated and six down-regulated phosphorylation sites, corresponding to 10 and six proteins, respectively, were identified in the insulin signalling pathway (FIGURE 4D–E). As insulin and glucagon function synergistically to sustain blood glucose homeostasis, and glucagon could increase intracellular cAMP levels and subsequently activate the activity of PKA, the up-regulation of insulin resistance and down-regulation of the glucagon signalling pathway in RPL secretory endometrium coincided with the previous proteome results that cyclic nucleotide signalling is changed (FIGURE 2).

Moreover, a PPI analysis comparing overall phosphorylation between RPL secretory endometrium and control secretory endometrium illustrated that the spliceosome was highly connected and centralized (FIGURE 4F). Additionally, most of the interacted spliceosomal proteins belong to the heterogeneous nuclear ribonucleoproteins or serine/arginine-rich proteins that regulate mRNA alternative splicing (*Hang et al., 2015*; *Li et al., 2020*). Remarkably, the spliceosome was also significantly altered for DPP in RPL proliferative endometrium compared with control proliferative endometrium by KEGG enrichment or PPI analysis (Supplementary Figure 4A–B), indicating that mRNA splicing may be aberrantly regulated in endometrium in both the secretory and proliferative phases in women with RPL.

Comprehensive interpretation of proteomic and phosphoproteomic profiles illustrate aberrations in both insulin and mTOR signalling

Next, the proteins that were dual-regulated were analysed in terms of expression level and PTM level. By searching the proteomic and phosphoproteomic datasets, eight overlapped proteins were identified in the RPL secretory endometrium versus control secretory endometrium comparison (FIGURE 5A). Amongst these, six were simultaneously over-expressed and hyper-phosphorylated, and the other two were down-regulated (FIGURE 5B). Intriguingly, as described previously, LPIN2 is involved in mTOR signalling (FIGURE 2C) and PRKAR1B is at the interface between cyclic nucleotide and insulin/PKA signalling (FIGURE 2D and FIGURE 4E); meanwhile, another PKA subunit, cAMP-dependent protein kinase catalytic subunit beta (PRKACB), was also hypo-phosphorylated (FIGURE 4E). Therefore, this study focused on insulin signalling and mTOR signalling for further validation.

The PKA kinase complex contains one catalytic subunit and four regulatory subunits (*Manning et al., 2002*), of which regulatory subunit PRKAR1B revealed dual-decreased protein expression and phosphorylation levels in RPL secretory endometrium, indicating that the activity of PKA is probably down-regulated. Western blot analysis of endometrial tissues in the secretory phase from a validation cohort of 10 independent patients indicated lower expression of PRKAR1B (FIGURE 5C and G), consistent with the proteomic data in this study. On the other hand, as ADCY3 functions upstream of PKA to produce cAMP, its increased expression may be due to a compensatory effect resulting from impaired PKA activity (FIGURE 5D and H). Meanwhile, in AMPK/mTOR signalling, the AMPK holoenzyme catalytic α subunit PRKAA2 is increased (FIGURE 5E and I), indicating up-regulated AMPK activity, thereby activating mTOR signalling. As a result, the phosphatidate phosphatase enzyme LPIN2 is also activated with over-expression (FIGURE 5F and J) and hyper-phosphorylation. A few exceptional cases are less consistent, most likely due to the presence of individual heterogeneity. By comprehensive interpretation of the proteomic and phosphoproteomic data, a regulatory model for secretory endometrium was proposed: increased insulin resistance down-regulates PKA activity, resulting in atypical cyclic nucleotide metabolism; and increased AMPK activity stimulates mTOR signalling, leading to aberrant triglyceride metabolism, causing secretory endometrial dysfunction and, ultimately, RPL (FIGURE 5K).

DISCUSSION

RPL is a frequently occurring disorder associated with female infertility, and its pathogenesis is closely related to dysfunction of the human endometrium (*Pirtea et al., 2021*). However, the cellular

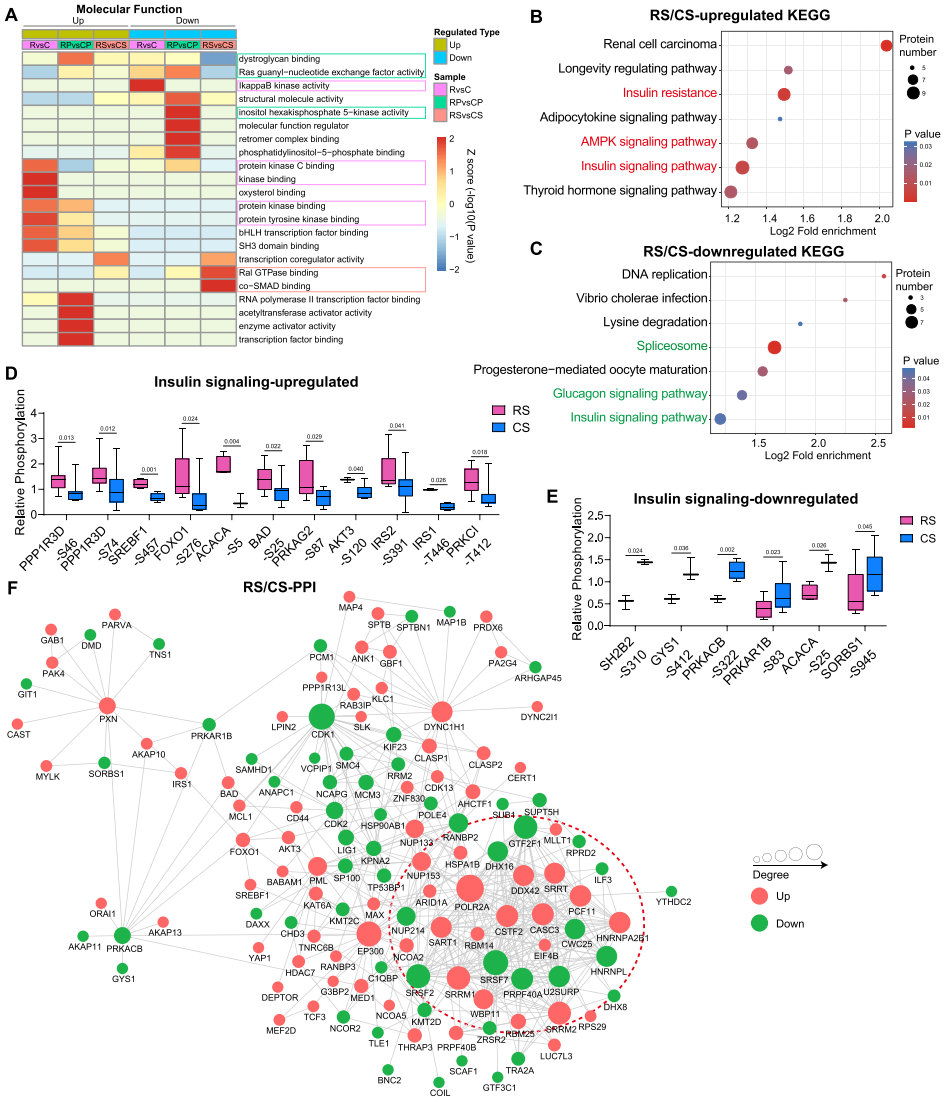

FIGURE 4 Phosphoproteomic analyses and protein–protein interaction (PPI). (A) Functional enrichment clustering analysis based on the molecular function (gene ontology category) of quantitative differentially phosphor-regulated proteins for up-regulation (celadon) and down-regulation (cyan). The kinase-related pathways are highlighted in coloured boxes with the box colour consistent with the sample type [R/C, recurrent pregnancy loss (RPL) endometrium/control endometrium; RP/CP, RPL proliferative endometrium/control proliferative endometrium; RS/CS, RPL secretory endometrium/control secretory endometrium]. Kyoto Encyclopedia of Genes and Genomes pathway enrichment of differentially phosphorylated proteins for (B) up-regulated and (C) down-regulated pathways in RS/CS comparison. The enriched phosphosites (given as protein–amino acid) in the insulin signalling pathway with (D) up-regulation and (E) down-regulation. The vertical axis is represented as an expression of Log2. The boxes represent the 25th and 75th percentiles, the central line marks the median value, and the whiskers show the upper and lower limits. (F) PPI network analysis of differentially phosphorylated proteins in RS/CS extracted from the STRING database. The dashed red circle indicates the spliceosomal-related proteins.

and molecular mechanisms underlying unexplained RPL remain poorly understood due to the complexity and diversity of its causes. Therefore, discernment of the detailed molecular underpinnings of RPL progression and exploration of novel therapeutic targets would greatly benefit women with RPL. This study presents the first proteomic-phosphoproteomic analysis of the endometrium of women with RPL, and identified dozens of DEP and hundreds of DPP between three comparison groups. The results demonstrated a sophisticated network in which proteins involved in the AMPK/mTOR signalling pathway and insulin signalling pathway were plausible in governing the regulation of function of the endometrium of women with RPL.

In contrast to the commonly used decidua, which is closely associated with miscarriage, this study used endometrial samples obtained from women with RPL who underwent hysteroscopic examination >3 months after their last miscarriage. The endometrium was considered to have recovered from the trauma caused by the miscarriage, and therefore the protein expression and phosphorylation pattern would be more reliable to reflect the baseline conditions of women with RPL. Nevertheless, due to the use of bulk endometrium instead of single-cell separation, it was not possible to distinguish endometrial cell types and attribute protein modifications to type-specific levels.

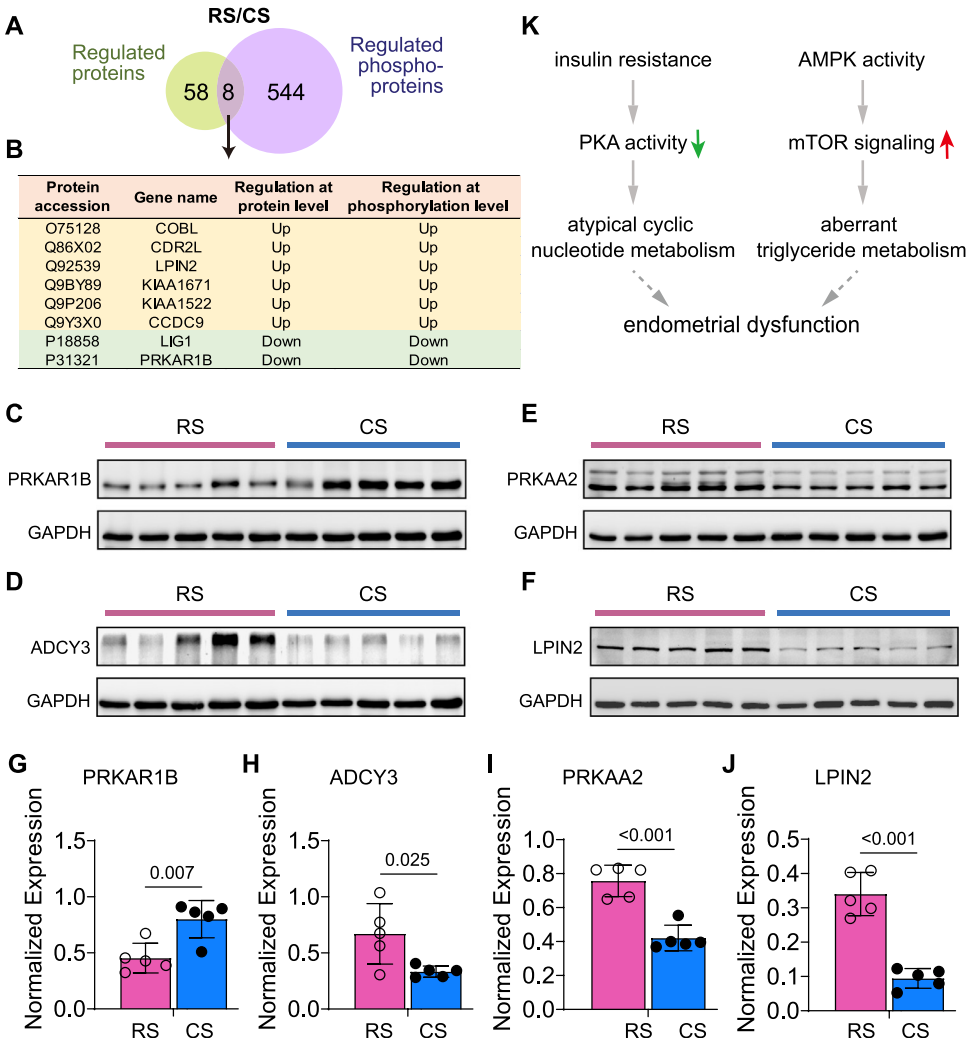

FIGURE 5 The combinative interpretation of proteome and phosphoproteome. (A) Venn diagram of the regulated proteins and regulated phosphoproteins. (B) Eight proteins were dual-regulated, with six of them being simultaneously over-expressed and hyper-phosphorylated and two of them being down-regulated and hypo-phosphorylated. Protein expression of (C) cAMP-dependent protein kinase type I-β regulatory subunit (PRKAR1B) (43 kDa), (D) adenylate cyclase type 3 (ADCY3) (129 kDa), (E) 5′-AMP-activated protein kinase catalytic subunit α-2 (PRKAA2) (62 kDa) and (F) phosphatidate phosphatase LPIN2 (LPIN2) (99 kDa) in the endometrial tissues of women with recurrent pregnancy loss (RPL) in the secretory phase (RS) and the endometrial tissues of control women in the secretory phase (CS) ($n = 5$ samples per group). Densitometric quantification of Western blot results for (G) PRKAR1B, (H) ADCY3, (I) PRKAA2 and (J) LPIN2, normalized to glyceraldehyde 3-phosphate dehydrogenase (GAPDH) expression. The data represent mean ± SD using Student's *t*-test. (K) Schematic diagram of the regulatory network in the endometrium of women with RPL.

Several previous studies have identified abnormal expression of endometrium-associated proteins in RPL. Endometrial biopsy tissue analysis has shown elevated expression of B-cell CLL/lymphoma 6 in women with RPL (*Fox et al., 2020*), and obese women with RPL have increased endometrial haptoglobin, an inflammatory marker associated with obesity (*Metwally et al., 2014*). Decorin and prostaglandin E2 receptor 3 both promote M1 macrophage polarization in decidua from early gestational miscarriages, and are strongly associated with the development of RPL (*Wang et al., 2022*; *Ye et al., 2022*). Together with the comprehensive proteomic and phosphoproteomic profiling from this study, these results suggest dysregulation of protein expression and regulation in the endometrium of women with RPL, which may affect embryonic development and pregnancy maintenance, leading to the development of RPL.

Furthermore, a higher prevalence of insulin resistance has been reported to be related to a history of RPL (*Craig et al., 2002*; *Maryam et al., 2012*), and insulin resistance has also been reported to increase the risk of spontaneous abortion after assisted reproductive technology treatment (*Tian et al., 2007*). This is consistent with the present discovery that the endometrium of women with RPL exhibits down-regulation of the insulin signalling pathway and the emergence of insulin resistance. Since PKA functions downstream of insulin signalling, the activation of PKA is essential for transcription of the decidual prolactin gene in human endometrial stromal cells (*Telgmann et al., 1997*). Within the PKA complex, PRKAR1B demonstrates dual down-regulation, affecting both protein expression (FIGURE 2D) and phosphorylation at residue Ser83 (PRKAR1B-S83, FIGURE 4E). In addition, the phosphorylation of another PKA protein, PRKACB, also experiences reduced levels at residue Ser322 (PRKACB-S322, FIGURE 4E). Alongside this,

the transcriptomic analysis of the human endometrium suggests a link between ADCY3 and progesterone-receptor-regulated stromal cell decidualization (*Mazur et al., 2015*).

Similarly, hyperactive mTOR signalling is closely related to abnormal endometrial function (*Bajwa et al., 2017*; *Guo and Yu, 2019*; *Rogers-Broadway et al., 2019*). LPIN2 is responsible for the penultimate step of triglyceride synthesis (*Zhang et al., 2016*), and is associated with progesterone-receptor-mediated decidualization (*Chi et al., 2020*). The present proteomic and experimental results display substantial activation of the endometrial mTOR signalling pathway in women with RPL during the secretory phase of the menstrual cycle. Additionally, AMPK, which consists of three subunits (α, β and γ) (*Kim and He, 2013*), is indispensable for post-parturition endometrial regeneration and tissue remodelling that accompanies decidualization (*McCallum et al., 2018*). Similar to the observed overexpression of PRKAA2 (**FIGURE 2C**), PRKAG2, the γ subunit of AMPK, presents up-regulated phosphorylation at residue Ser87 (PRKAG2-S87) in women with RPL (**FIGURE 4D**). All of these observations suggest potential correlation between the aberrant inhibition of PKA and/or activation of AMPK with the pathogenesis of RPL. However, further investigation is required to elucidate the underlying regulatory network.

Additionally, it is reported that collagen type VI is abundant in human endometrium during the proliferative phase, but gradually disappears in the secretory phase (*Uitto and Larjava, 1991*), and collagen type VI is lost from rat stromal cells undergoing decidualization (*Mulholland et al., 1992*). Therefore, the abnormal increase in collagen deposition in all three categories suggests that excessive accumulation of structural components of extracellular matrix fractions in the proliferative phase may impair endometrial function in women with RPL.

To investigate the datasets more systematically and to explore the potential kinase targets, kinase activity prediction was undertaken based on the substrate phosphorylation differences tailored for the phosphoproteomic profile. Among the putatively activated kinases, Rho-associated protein kinase 1 (ROCK1) showed significant positive regulation in RPL secretory endometrium compared with control secretory endometrium (Supplementary Figure 5A and C). ROCK1 inhibits the proliferation and migration of human chorionic trophoblast HTR-8/Svneo cells and promotes apoptosis (*Ma et al., 2020*). Therefore, activated ROCK1 in RPL secretory endothelium may result in reduced endometrial proliferation and influence normal decidualization and fetal implantation, leading to the occurrence of RPL. Casein kinase II subunit α (CK2A1) and casein kinase II subunit α' (CK2A2) are two subunits of casein kinase II (*Yang-Feng et al., 1991*), whose opposing behaviours in RPL secretory endometrium and RPL proliferative endometrium demonstrated the differential regulatory function of casein kinase II in menstrual phases (Supplementary Figure S5A–D). Furthermore, kinase-pathway network analysis was used for the phosphoproteomic data to gain insights into the phosphorylation network. Interestingly, ROCK1, CK2A1 and CK2A2 were found to be located at the hub of the enriched KEGG pathway network in RPL secretory endometrium compared with control secretory endometrium (Supplementary Figure 6). The results enhance understanding of the relationship between phosphorylated kinase and substrate modification. All these alterations will be validated in a further study.

In conclusion, although it is not possible to conclude whether or not these alterations would cause RPL due to the lack of cellular and animal validation (the authors are currently investigating how aberrant insulin resistance and mTOR signalling are connected to RPL), this comprehensive analysis of differential protein expression and phosphorylation profiles of RPL endometrium reveals dysregulation of insulin/cAMP and AMPK/mTOR signalling in the endometrium of women with RPL. These findings help to explain the mechanisms underlying the unexplained pathogenesis of RPL.

DATA AVAILABILITY

Data will be made available on request.

AUTHOR CONTRIBUTIONS

This work was performed by all authors. J. H. and X. Z. conceived and designed the study; C.C., F.D. and Q.W. collected the tissues and performed the experiments; J. H. and C.C. performed the data analysis and wrote the manuscript; and R.L. and Y. W. contributed to the sample collection and data analysis.

FUNDING

This work was supported by the National Key Research and Development Programme of China (2022YFC2702904), the National Natural Science Foundation of China (Nos. 82071658, 81802689 and 81701537), the Beijing Nova Programme (20220484160), the Key Laboratory of Assisted Reproduction (Peking University), the Ministry of Education (BYSYSZKF2022004), and the National Key Research and Development Program of China (2016YFC1000302).

SUPPLEMENTARY MATERIALS

Supplementary material associated with this article can be found in the online version at doi:10.1016/j.rbmo.2023.103585.

REFERENCES

Alecsandru, D., Klimczak, A.M., Garcia Velasco, J.A., Pirtea, P., Franasiak, J.M., 2021. Immunologic causes and thrombophilia in recurrent pregnancy loss. Fertil. Steril. 115, 561–566.

Bahia, W., Soltani, I., Abidi, A., Haddad, A., Ferchichi, S., Menif, S., Almawi, W.Y., 2020. Identification of genes and miRNA associated with idiopathic recurrent pregnancy loss: an exploratory data mining study. BMC Med. Genomics 13, 75.

Bajwa, P., Nielsen, S., Lombard, J.M., Rassam, L., Nahar, P., Rueda, B.R., Wilkinson, J.E., Miller, R.A., Tanwar, P.S., 2017. Overactive mTOR signaling leads to endometrial hyperplasia in aged women and mice. Oncotarget. 8, 7265–7275.

Bruno, V., Lindau, R., Jenmalm, M.C., Ticconi, C., Piccione, E., Pietropolli, A., Ernerudh, J., 2020. First-trimester trophoblasts obtained by chorionic villus sampling maintain tolerogenic and proteomic features in successful pregnancies despite a history of unexplained recurrent pregnancy loss. Am. J. Reprod. Immunol. 84, e13314.

Carbonnel, M., Pirtea, P., de Ziegler, D., Ayoubi, J.M., 2021. Uterine factors in recurrent pregnancy losses. Fertil. Steril. 115, 538–545.

Chen, P., Zhou, L., Chen, J., Lu, Y., Cao, C., Lv, S., Wei, Z., Wang, L., Chen, J., Hu, X., Wu, Z., Zhou, X., Su, D., Deng, X., Zeng, C., Wang, H., Pu, Z., Diao, R., Mou, L., 2021. The Immune Atlas of Human Deciduas With Unexplained Recurrent Pregnancy Loss. Front. Immunol. 12, 689019.

Chi, R.A., Wang, T., Adams, N., Wu, S.P., Young, S.L., Spencer, T.E., DeMayo, F., 2020. Human Endometrial Transcriptome and Progesterone Receptor Cistrome Reveal Important Pathways and Epithelial Regulators. J. Clin. Endocrinol. Metab. 105, e1419–e1439.

Craig, L.B., Ke, R.W., Kutteh, W.H., 2002. Increased prevalence of insulin resistance in women with a history of recurrent pregnancy loss. Fertil. Steril. 78, 487–490.

Critchley, H.O.D., Maybin, J.A., Armstrong, G.M., Williams, A.R.W., 2020. Physiology of the Endometrium and Regulation of Menstruation. Physiol. Rev. 100, 1149–1179.

de Ziegler, D., Frydman, R.F., 2021. Recurrent pregnancy losses, a lasting cause of infertility. Fertil. Steril. 115, 531–532.

Dhaenens, L., Lierman, S., De Clerck, L., Govaert, E., Deforce, D., Tilleman, K., De Sutter, P., 2019. Endometrial stromal cell proteome mapping in repeated implantation failure and recurrent pregnancy loss cases and fertile women. Reprod. Biomed. Online 38, 442–454.

Dimitriadis, E., Menkhorst, E., Saito, S., Kutteh, W.H., Brosens, J.J., 2020. Recurrent pregnancy loss. Nat. Rev. Dis. Primers 6, 98.

El Hachem, H., Crepaux, V., May-Panloup, P., Descamps, P., Legendre, G., Bouet, P.E., 2017. Recurrent pregnancy loss: current perspectives. Int. J. Womens Health 9, 331–345.

ESHRE Guideline Group on, RPL, Bender Atik, R., Christiansen, O.B., Elson, J., Kolte, A.M., Lewis, S., Middeldorp, S., Nelen, W., Peramo, B., Quenby, S., Vermeulen, N., Goddijn, M., 2018. ESHRE guideline: recurrent pregnancy loss. Hum. Reprod. Open. 2018, hoy004.

Fox, C.W., Savaris, R.F., Jeong, J.W., Kim, T.H., Miller, P.B., Likes, C.E., Schammel, D.P., Young, S.L., Lessey, B.A., 2020. Unexplained recurrent pregnancy loss and unexplained infertility: twins in disguise. Hum. Reprod. Open. 2020, hoz021.

Gellersen, B., Brosens, J.J., 2014. Cyclic decidualization of the human endometrium in reproductive health and failure. Endocr. Rev. 35, 851–905.

Guo, C., Cai, P., Jin, L., Sha, Q., Yu, Q., Zhang, W., Jiang, C., Liu, Q., Zong, D., Li, K., Fang, J., Lu, F., Wang, Y., Li, D., Lin, J., Li, L., Zeng, Z., Tong, X., Wei, H., Qu, K., 2021. Single-cell profiling of the human decidual immune microenvironment in patients with recurrent pregnancy loss. Cell. Discov. 7, 1.

Guo, Z., Yu, Q., 2019. Role of mTOR Signaling in Female Reproduction. Front. Endocrinol. (Lausanne) 10, 692.

Hang, J., Wan, R., Yan, C., Shi, Y., 2015. Structural basis of pre-mRNA splicing. Science 349, 1191–1198.

Hua, H., Kong, Q., Zhang, H., Wang, J., Luo, T., Jiang, Y., 2019. Targeting mTOR for cancer therapy. J. Hematol. Oncol. 12, 71.

Huang, C., Zeng, Y., Tu, W., 2021. Single-cell RNA Sequencing Deciphers Immune Landscape of Human Recurrent Miscarriage. Genomics Proteomics Bioinformatics 19, 169–171.

Jauniaux, E., Farquharson, R.G., Christiansen, O.B., Exalto, N., 2006. Evidence-based guidelines for the investigation and medical treatment of recurrent miscarriage. Hum. Reprod. 21, 2216–2222.

Kim, I., He, Y.Y., 2013. Targeting the AMP-Activated Protein Kinase for Cancer Prevention and Therapy. Front. Oncol. 3, 175.

Klimczak, A.M., Patel, D.P., Hotaling, J.M., Scott, Jr., R.T., 2021. Role of the sperm, oocyte, and embryo in recurrent pregnancy loss. Fertil. Steril. 115, 533–537.

Kumar, L., Futschik, M.E., 2007. Mfuzz: a software package for soft clustering of microarray data. Bioinformation 2, 5–7.

Li, J., Lu, M., Zhang, P., Hou, E., Li, T., Liu, X., Xu, X., Wang, Z., Fan, Y., Zhen, X., Li, R., Liu, P., Yu, Y., Hang, J., Qiao, J., 2020. Aberrant spliceosome expression and altered alternative splicing events correlate with maturation deficiency in human oocytes. Cell Cycle 19, 2182–2194.

Ma, X.L., Li, X., Tian, F.J., Zeng, W.H., Zhang, J., Mo, H.Q., Qin, S., Sun, L.Q., Zhang, Y.C., Zhang, Y., Lin, Y., 2020. Upregulation of RND3 Affects Trophoblast Proliferation, Apoptosis, and Migration at the Maternal-Fetal Interface. Front. Cell. Dev. Biol. 8, 153.

Manning, G., Whyte, D.B., Martinez, R., Hunter, T., Sudarsanam, S., 2002. The protein kinase complement of the human genome. Science 298, 1912–1934.

Maryam, K., Bouzari, Z., Basirat, Z., Kashifard, M., Zadeh, M.Z., 2012. The comparison of insulin resistance frequency in patients with recurrent early pregnancy loss to normal individuals. BMC Res. Notes 5, 133.

Mazur, E.C., Vasquez, Y.M., Li, X., Kommagani, R., Jiang, L., Chen, R., Lanz, R.B., Kovanci, E., Gibbons, W.E., DeMayo, F.J., 2015. Progesterone receptor transcriptome and cistrome in decidualized human endometrial stromal cells. Endocrinology 156, 2239–2253.

McCallum, M.L., Pru, C.A., Smith, A.R., Kelp, N.C., Foretz, M., Viollet, B., Du, M., Pru, J.K., 2018. A functional role for AMPK in female fertility and endometrial regeneration. Reproduction 156, 501–513.

Metwally, M., Preece, R., Thomas, J., Ledger, W., Li, T.C., 2014. A proteomic analysis of the endometrium in obese and overweight women with recurrent miscarriage: preliminary evidence for an endometrial defect. Reprod. Biol. Endocrinol. 12, 75.

Mulholland, J., Aplin, J.D., Ayad, S., Hong, L., Glasser, S.R., 1992. Loss of collagen type VI from rat endometrial stroma during decidualization. Biol. Reprod. 46, 1136–1143.

Naglot, S., Tomar, A.K., Singh, N., Yadav, S., 2021. Label-free proteomics of spermatozoa identifies candidate protein markers of idiopathic recurrent pregnancy loss. Reprod. Biol. 21, 100539.

Pfleger, J., Gresham, K., Koch, W.J., 2019. G protein-coupled receptor kinases as therapeutic targets in the heart. Nat. Rev. Cardiol. 16, 612–622.

Pirtea, P., Cicinelli, E., De Nola, R., de Ziegler, D., Ayoubi, J.M., 2021. Endometrial causes of recurrent pregnancy losses: endometriosis, adenomyosis, and chronic endometritis. Fertil. Steril. 115, 546–560.

Rogers-Broadway, K.R., Kumar, J., Sisu, C., Wander, G., Mazey, E., Jeyaneethi, J., Pados, G., Tsolakidis, D., Klonos, E., Grunt, T., Hall, M., Chatterjee, J., Karteris, E., 2019. Differential expression of mTOR components in endometriosis and ovarian cancer: Effects of rapalogues and dual kinase inhibitors on mTORC1 and mTORC2 stoichiometry. Int. J. Mol. Med. 43, 47–56.

Salamonsen, L.A., 2019. Women in reproductive science: My WOMBan's life: understanding human endometrial function. Reproduction 158, F55–F67.

Salker, M., Teklenburg, G., Molokhia, M., Lavery, S., Trew, G., Aojanepong, T., Mardon, H.J., Lokugamage, A.U., Rai, R., Landles, C., Roelen, B.A., Quenby, S., Kuijk, E.W., Kavelaars, A., Heijnen, C.J., Regan, L., Macklon, N.S., Brosens, J.J., 2010. Natural selection of human embryos: impaired decidualization of endometrium disables embryo-maternal interactions and causes recurrent pregnancy loss. PLoS One 5, e10287.

Tarrant, M.K., Cole, P.A., 2009. The chemical biology of protein phosphorylation. Annu. Rev. Biochem. 78, 797–825.

Telgmann, R., Maronde, E., Tasken, K., Gellersen, B., 1997. Activated protein kinase A is required for differentiation-dependent transcription of the decidual prolactin gene in human endometrial stromal cells. Endocrinology 138, 929–937.

Tian, L., Shen, H., Lu, Q., Norman, R.J., Wang, J., 2007. Insulin resistance increases the risk of spontaneous abortion after assisted reproduction technology treatment. J. Clin. Endocrinol. Metab. 92, 1430–1433.

Uitto, V.J., Larjava, H., 1991. Extracellular matrix molecules and their receptors: an overview with special emphasis on periodontal tissues. Crit. Rev. Oral. Biol. Med. 2, 323–354.

Vlahou, A., Fountoulakis, M., 2005. Proteomic approaches in the search for disease biomarkers. J. Chromatogr. B. Analyt. Technol. Biomed. Life Sci. 814, 11–19.

Wang, F., Jia, W., Fan, M., Shao, X., Li, Z., Liu, Y., Ma, Y., Li, Y.X., Li, R., Tu, Q., Wang, Y.L., 2021.

Single-cell Immune Landscape of Human Recurrent Miscarriage. Genomics Proteomics Bioinformatics 19, 208–222.
Wang, L., Wang, H., Luo, J., Xie, T., Mor, G., Liao, A., 2022. Decorin promotes decidual M1-like macrophage polarization via mitochondrial dysfunction resulting in recurrent pregnancy loss. Theranostics 12, 7216–7236.
Xiong, Y.M., Pan, H.T., Ding, H.G., He, Y., Zhang, J., Zhang, F., Yu, B., Zhang, T., Huang, H.F., 2021. Proteomic and functional analysis of proteins related to embryonic development of decidua in patients with recurrent pregnancy loss. Biol. Reprod. 105, 1246–1256.
Xue, D., Zhang, Y., Wang, Y., Wang, J., An, F., Sun, X., Yu, Z., 2019. Quantitative proteomic analysis of sperm in unexplained recurrent pregnancy loss. Reprod. Biol. Endocrinol. 17, 52.
Yang-Feng, T.L., Zheng, K., Kopatz, I., Naiman, T., Canaani, D., 1991. Mapping of the human casein kinase II catalytic subunit genes: two loci carrying the homologous sequences for the alpha subunit. Nucleic. Acids. Res. 19, 7125–7129.
Ye, Y., Peng, L., Chelariu-Raicu, A., Kuhn, C., Dong, X., Jeschke, U., von Schonfeldt, V., 2022. Prostaglandin E2 receptor 3 promotes M1 macrophages polarization in unexplained recurrent pregnancy loss. Biol. Reprod. 106, 910–918.
Yin, X.J., Hong, W., Tian, F.J., Li, X.C., 2021. Proteomic analysis of decidua in patients with recurrent pregnancy loss (RPL) reveals mitochondrial oxidative stress dysfunction. Clin. Proteomics 18, 9.
Yu, M., Du, G., Xu, Q., Huang, Z., Huang, X., Qin, Y., Han, L., Fan, Y., Zhang, Y., Han, X., Jiang, Z., Xia, Y., Wang, X., Lu, C., 2018. Integrated analysis of DNA methylome and transcriptome identified CREB5 as a novel risk gene contributing to recurrent pregnancy loss. EBioMedicine. 35, 334–344.
Zhang, X., Fu, L.J., Liu, X.Q., Hu, Z.Y., Jiang, Y., Gao, R.F., Feng, Q., Lan, X., Geng, Y.Q., Chen, X.M., He, J.L., Wang, Y.X., Ding, Y.B., 2016. nm23 regulates decidualization through the PI3K-Akt-mTOR signaling pathways in mice and humans. Hum. Reprod. 31, 2339–2351.
Zhou, L., Pu, Y., Zhou, Y., Wang, B., Chen, Y., Bai, Y., He, S., 2021. Genome wide methylation analysis to uncover genes related to recurrent pregnancy loss. Genes Genomics 43, 361–369.

Received 13 May 2023; received in revised form 15 September 2023; accepted 27 September 2023.